

Article

Pristine and UV-Weathered PET Microplastics as Water Contaminants: Appraising the Potential of the Fenton Process for Effective Remediation

Marin Kovačić ¹, Antonija Tomić ¹, Stefani Tonković ¹, Anamarija Pulitika ¹ , Josipa Papac Zjačić ¹, Zvonimir Katančić ¹ , Boštjan Genorio ² , Hrvoje Kušić ¹ and Ana Lončarić Božić ^{1,*}

¹ Faculty of Chemical Engineering and Technology, University of Zagreb, Trg Marka Marulića 19, HR-10000 Zagreb, Croatia; mkovacic@fkit.unizg.hr (M.K.); atomic@fkit.unizg.hr (A.T.); stonkovic@fkit.unizg.hr (S.T.); pulitika@fkit.unizg.hr (A.P.); jpapac@fkit.unizg.hr (J.P.Z.); katanacic@fkit.unizg.hr (Z.K.); hkusic@fkit.unizg.hr (H.K.)

² Faculty of Chemistry and Chemical Technology, University of Ljubljana, Večna pot 113, SI-1000 Ljubljana, Slovenia; bostjan.genorio@fkt.uni-lj.si

* Correspondence: abozic@fkit.unizg.hr

Abstract: Polyethylene terephthalate (PET) microplastics constitute a significant portion of plastic pollution in the environment and pose substantial environmental challenges. In this study, the effectiveness of the Fenton process and post-oxidation coagulation for the removal of non-weathered and UV-weathered PET microplastics (PET MPs) were investigated. A response surface methodology was used to investigate the interplay between PET concentration and ferrous ion (Fe²⁺) concentration. The models revealed an intricate interplay between these variables, highlighting the need for a balanced system for optimal PET MP removal. For non-weathered PET, the simultaneous increase in the concentrations of both PET microplastics and Fe²⁺ was found to enhance the removal efficiency. However, this synergistic effect was not observed in UV-weathered PET, which also demonstrated a more pronounced effect from the Fe²⁺ concentration. The statistical analysis provided a strong basis for the validity of the models. X-ray photoemission spectroscopy (XPS) further elucidated the mechanisms behind these findings, revealing that UV weathering results in surface changes, which facilitate hydroxyl radical oxidation. These findings underline the complexity of the Fenton process in PET microplastic removal and the different behavior of non-weathered and UV-weathered microplastics. This has significant implications for tailoring remediation strategies and underscores the importance of considering environmental weathering in these strategies.

Keywords: Fenton process; microplastics; oxidation; polyethylene terephthalate; removal; weathering



Citation: Kovačić, M.; Tomić, A.; Tonković, S.; Pulitika, A.; Papac Zjačić, J.; Katančić, Z.; Genorio, B.; Kušić, H.; Lončarić Božić, A. Pristine and UV-Weathered PET Microplastics as Water Contaminants: Appraising the Potential of the Fenton Process for Effective Remediation. *Processes* **2024**, *12*, 844. <https://doi.org/10.3390/pr12040844>

Academic Editors: Nediljka Vukojevic Medvidovic, Ladislav Vrsalović and Emeka Emmanuel Oguzie

Received: 27 March 2024

Revised: 19 April 2024

Accepted: 20 April 2024

Published: 22 April 2024



Copyright: © 2024 by the authors. Licensee MDPI, Basel, Switzerland. This article is an open access article distributed under the terms and conditions of the Creative Commons Attribution (CC BY) license (<https://creativecommons.org/licenses/by/4.0/>).

1. Introduction

Microplastics (MPs), tiny plastic fragments less than 5 mm in size, are ubiquitous pollutants that pose a significant threat to aquatic environments globally [1]. MPs can be divided into primary and secondary MPs, i.e., those that are primarily produced at this size and those that are a result of the fragmentation of larger plastic materials. Over time, due to wear and tear, plastic materials break down into smaller particles that can enter the environment. One of the most common plastic materials used worldwide is polyethylene terephthalate (PET), which is a clear, strong, and lightweight plastic widely used in beverage bottles and food packaging. It is also used in synthetic fibers for clothing (i.e., polyester), thermoformed packaging, and in combination with glass fiber for engineered resins. These applications, while beneficial for various industries, contribute substantially to plastic waste and, subsequently, to the increasing presence of PET microplastics in aquatic environments. According to Plastics Europe, Worldwide production of PET was 24.2 million metric tons in 2021 and constituted 6.2% of produced plastics [2]. PET production has been increasing

over time, driven by rising global demand. Due to its widespread use and often improper disposal, PET is ubiquitous in the environment and represents a persistent pollutant [3]. PET can end up in the food chain due to ingestion from a range of organisms in the environment, ranging from small zooplankton to larger aquatic and terrestrial animals. Ingestion of MPs, in general, can cause harm to organisms, such as physical harm due to blockage in the digestive tract, accumulation in the gills of fish, and increased cellular oxidative stress [4–8]. In addition, MPs can transport pollutants within the ecosystem. Worryingly, microplastics, and PET in particular, can end up in water and food for human consumption. In a study conducted by Adediran et al. [9], PET MPs have been detected in 45% of drinking water samples and are one of the most prevalent MPs in wastewater effluents. PET MPs have been detected in skim milk powders [10], canned seafood [11], table salt [12], and others [13]. Previous studies have shown that microplastics can absorb harmful pollutants, commonly known as persistent organic pollutants (POPs), and can vector them through the environment. In addition, MPs can also act as vectors for invasive species and pathogens [14–16]. The surface properties of microplastics often change when exposed to environmental factors like UV radiation. Such weathering or aging can alter their behavior in the aquatic environment [7,8]. UV weathering of microplastics, a primary environmental factor affecting the properties and behavior of these materials, causes photo-oxidative degradation, which modifies the physico-chemical characteristics of the plastic particles by introducing oxygen-containing moieties (hydroxyl or carboxyl groups). This, in turn, enhances the potential of MPs to adsorb POPs and can affect the release rates [17]. Additionally, these alterations may change the way marine organisms interact with microplastics, influencing their ingestion rates [15].

Since PET has a higher density than freshwater and seawater, unlike many other MPs, it should theoretically be less buoyant and, hence, less mobile in the aquatic environment. Presumably, this is one of the reasons why PET microplastics are somewhat less studied than, e.g., polyethylene (PE). A search on Scopus on 25 March 2024 with the keywords “polyethylene AND microplastic*” returned 5856 results, whereas “terephthalate AND microplastic*” returned 2393 results. On the other hand, PET is likely more prone to accumulate in the sediment and thus affect benthic organisms to a greater extent.

The investigation of wastewater treatment technologies to prevent the release of MPs, including PET, is of great importance. Wastewater treatment plants (WWTPs) are considered a major source of microplastic pollution in the environment. Microplastics, including PET, enter the wastewater influent through various means, such as during mechanical abrasion of fibers during washing of synthetic clothes, the breakdown of larger plastic items, and from personal care products that contain microbeads. While many WWTPs are designed to remove larger debris and particles, they may not effectively remove smaller microplastic particles [18].

Hence, the study of effective removal methods for PET from wastewater is of great importance. Currently, a small body of research on the applicability of AOPs for the degradation of microplastics exists [19,20]. A potential solution is the Fenton process, a well-established advanced oxidation process (AOP) used for the degradation of organic pollutants in water and wastewater. It involves the generation of hydroxyl radicals ($\bullet\text{OH}$) through the reaction of hydrogen peroxide (H_2O_2) with ferrous iron (Fe^{2+}) as a catalyst at favorable acidic pH. These hydroxyl radicals are extremely potent and unselective oxidants that can degrade a wide variety of organic compounds [21,22]. Oxidative damage to the polymer chains can lead to the breakdown of the microplastic particles into smaller fragments or even potentially complete mineralization into CO_2 and H_2O for certain types of plastics [19]. Fenton is a highly attractive AOP for this purpose, as, upon expending H_2O_2 , residual ferric (Fe^{3+}) species need to be removed. Commonly, this is performed by neutralization of the reaction solution, whereby conditions conducive to coagulation occur. In a typical Fenton process for the degradation of other, less persistent pollutants—the ferric sludge is considered to be a problematic aspect. However, the growing particles of

hydrated iron oxides can act as a coagulation agent that can entrap and remove particulate matter, i.e., microplastics, from water.

In this study, the effectiveness of the Fenton process and post-oxidation coagulation with the residual ferric ions on the removal of PET MPs from water was studied.

2. Materials and Methods

2.1. Chemicals

Iron(II) sulfate heptahydrate ($\text{FeSO}_4 \times 7\text{H}_2\text{O}$, >99.0%, Sigma-Aldrich, Saint Louis, MO, USA) and hydrogen peroxide (H_2O_2 , $w = 30\%$, T.T.T., Sveta Nedjelja, Croatia) were used as Fenton reagents. Polyethylene terephthalate granules were obtained from Sigma Aldrich (Saint Louis, MO, USA); 0.1 M sulfuric acid (H_2SO_4 , p.a., Lach-Ner, Neratovice, Czech Republic) and 0.1 M sodium hydroxide (NaOH, p.a., Lach-Ner, Neratovice, Czech Republic) were used for pH adjustments. Orthophosphoric acid (H_3PO_4 , $w = 85\%$, Honeywell Fluka, Charlotte, NC, USA) was used for solid sample total organic content (TOC) analysis. The aqueous solutions were prepared with ultra-pure water ($>18.0 \text{ M}\Omega \times \text{cm}$) obtained using a Direct-Q3 UV (Merck Millipore, Darmstadt, Germany) ultra-pure water system.

2.2. Preparation of PET MP Samples

The PET granules were first formed into 0.12 mm thick sheets via hot press model 44–226 (Dake Corporation, Grand Haven, MI, USA). One sheet was exposed to UV irradiation in a Suntest CPS weathering chamber (Heraeus, Hanau, Germany) equipped with a xenon arc lamp for 28 days continuously. The weathered material is referred to as PET_{28} , whereas the pristine materials are denoted as PET_0 . The obtained sheets were then cut up into smaller pieces and ground into microplastics by cryogenic ball milling. For this purpose, a CryoMill (Retsch, Haan, Germany) was programmed to grind the samples using the following conditions: (i) precooling ($f = 5 \text{ s}^{-1}$; $t = 1 \text{ min}$), (ii) grinding ($f = 25 \text{ s}^{-1}$; $t = 1 \text{ min}$), followed by intercooling between every grinding cycle ($f = 5 \text{ s}^{-1}$; $t = 30 \text{ s}$) [23]. Liquid nitrogen (Uljanik tehnički plinovi, Pula, Croatia) was used during the milling process. After milling, the obtained samples were sieved into 100–500 μm fractions using an AS 200 mechanical sieve shaker (Retsch, Haan, Germany).

2.3. MP Removal by Fenton Process

The effectiveness of the Fenton process for the removal of PET MPs from water was investigated using the statistical experimental design approach. The mass concentration of the PET MPs, denoted as coded variable X_1 , and the concentration of Fe^{2+} , denoted as X_2 , were varied. pH and the concentration of H_2O_2 were fixed at pH = 4 and $[\text{H}_2\text{O}_2] = 80 \text{ mM}$, respectively. A three-level-factorial experimental plan (3^2) was chosen, where the individual levels of the variable X_1 were 125 ppm, 250 ppm, and 375 ppm, whereas the values for X_2 were 10 mM, 25 mM, and 40 mM, as shown in Table 1. Design-Expert 10.1 (StatEase, Minneapolis, MN, USA) and Statistica 13.5 (Tibco, München, Germany) software were used to analyze the obtained data and perform response surface modeling and analysis of variance (ANOVA). The experiments were conducted by first weighing the required amount of PET MPs, as per experimental run, and transferring the MPs quantitatively to tall 150 mL beakers, to which a 20 mm \times 6 \times mm stir bar was previously added. The ratio of the length of the stir bar and the diameter of the beakers was approximately 1:2.7. Then, 100 mL of a freshly made solution containing ferrous ions at the designated concentration according to the experimental plan was added, and the pH was adjusted to pH 4. To this solution, the required amount of H_2O_2 was added, which was considered to be the beginning of the experiment. For the first 30 min, the suspension was stirred at 450 rpm, after which the pH was increased to 8.5 in order to quench the reaction and initiate precipitation of the hydrated iron oxide species. The reaction mixture was stirred then at 100 rpm for a further 30 min. Then, the stirring was stopped, and the particles were allowed to settle out for a duration of 24 h. All experiments were performed in triplicate in order to ensure higher reproductivity of results.

Table 1. Experimental design used in the study, with the corresponding levels of the variables.

Parameters	Model Variables/Coded Values	Level/Range		
		−1	0	1
γ (MP), mg L ^{−1}	X ₁	5	20	35
[Fe ²⁺], mM	X ₂	10	25	40

2.4. Quantification of the PET MP Removal

After the sedimentation process, the supernatant was decanted, and the wet ferric sludge was carefully filtered through a quartz fiber filter paper (Whatman QM-H, $r = 37$ mm). The obtained filter cake was dried for 24 h at 80 °C. The dried filter cake, containing the entrained PET MPs, was homogenized using an agate pestle and mortar. Then, 20.0 ± 0.5 mg of the dried sample was weighed out in a ceramic sample boat for solid-state TOC analysis. The ceramic sample boats were calcined beforehand at 900 °C for 30 min in an electric muffle furnace (LP-07, Instrumentaria, Zagreb, Croatia) to remove any residual organic or inorganic carbon. The samples were acidified with a few drops of 0.8 M H₃PO₄ in order to convert inorganic carbon in the form of carbonates to carbon dioxide. The acidified samples were then placed in a DZF-6020 vacuum oven (Lenphan, Zhengzhou, China) heated to 60 °C and evacuated to 0.8 atm for 30 min to outgas evolved CO₂. This was performed so as not to include inorganic carbon content during the quantification of the total organic carbon content in the samples, which originates from the PET MPs. After the inorganic carbon was removed, the treated samples were analyzed using TOC-V CPN analyzer (Shimadzu, Kyoto, Japan) coupled with a solid sample combustion unit SSM-5000A (Shimadzu, Kyoto, Japan). The combustion furnace of the solid sample unit was heated to 900 °C. Pristine PET MPs were used as a standard to obtain the calibration of the instrument's response. The measured total organic carbon of the samples was corrected for the measured carbon content in 0.8 M H₃PO₄, i.e., the blank sample. The removal of the PET microplastic was determined based on the hypothesized total removal of the PET MPs (TOC_{theoretical}), i.e., by measuring the total organic carbon content of the PET sample weigh-outs, Equation (1):

$$\text{removal efficiency}(\%) = 100 - \left(\frac{\text{TOC}_{\text{sample}}}{\text{TOC}_{\text{theoretical}}} \right) \times 100 \quad (1)$$

All measurements were performed in triplicates; thus, for each experimental point, we had 9 results (3 replicates \times 3 measurements); averages with high reproducibility (97.4%) are reported.

2.5. X-ray Photoemission Spectroscopy Characterization

In order to assess the effects of the Fenton treatment on the functional groups on the surface of microplastics, X-ray photoemission spectroscopy (XPS) analysis of the samples was performed. The samples were placed onto adhesive graphite tapes and were analyzed without a pre-treatment to coat the samples with a conductive layer by vapor phase deposition. A PHI VersaProbe III (Version AD) (PHI, Chanhassen, MN, USA) equipped with a hemispherical analyzer and an Al K α monochromatic X-ray source were used. Survey spectra were recorded using 224 eV pass energy at a step of 0.8 eV, whereas Fe 2p core level spectra were analyzed at a pass energy of 27 eV at a step of 0.1 eV. Data acquisition was performed with ESCApe 1.4 software. The fitting of the C 1s and Fe 2p level spectra was performed using CasaXPS 2.3.15. software.

3. Results and Discussion

3.1. Removal of PET MPs by the Fenton Process

The aim of this study was to model the removal efficiency of pristine and UV-weathered polyethylene terephthalate (PET) microplastics using the Fenton process and

post-Fenton coagulation facilitated by the precipitation of ferric species. The model parameters under consideration were the concentrations of the pristine (PET₀) and weathered (PET₂₈) PET microplastics (X₁) and ferrous ions (Fe²⁺) (X₂) as the catalyst for the Fenton reaction, while the concentration of H₂O₂ was kept constant. Response surface methodology (RSM) was used to generate a second-order polynomial model for the removal efficiency (Y₁) by applying the multiple regression analysis on the full factorial matrix and corresponding experimental results, i.e., removal extents, presented in Table S1 (Supplementary Information). In such a way, a complex relationship between the removal of PET microplastics and the designated variables was revealed and presented as 3D-surface plots (Figure 1). In order to successfully apply RSM for the intended action, the first postulate is to have accurate, significant, and predictive models. Usually, RSM models are evaluated on the basis of analysis of variance (ANOVA), an essential test providing a list of statistical parameters such as: Fisher F-test value (*F*), its probability value (*p*), regression coefficients (pure; *R*², adjusted; *R*_{adj}², predicted; *R*_{pre}²), t-test value, etc. Most commonly, initial screening of model significance and accuracy may be provided through pertaining *p*, *R*², and *R*_{adj}² values [24–26]. The corresponding response surface model equation (Y₁) for the removal of pristine PET MPs is shown in Equation (2):

$$Y_1 = 15.31 - 7.30X_1 - 5.34 X_2 + 6.31 X_1 \times X_2 + 25.57X_1^2 + 5.75X_2^2 \quad (2)$$

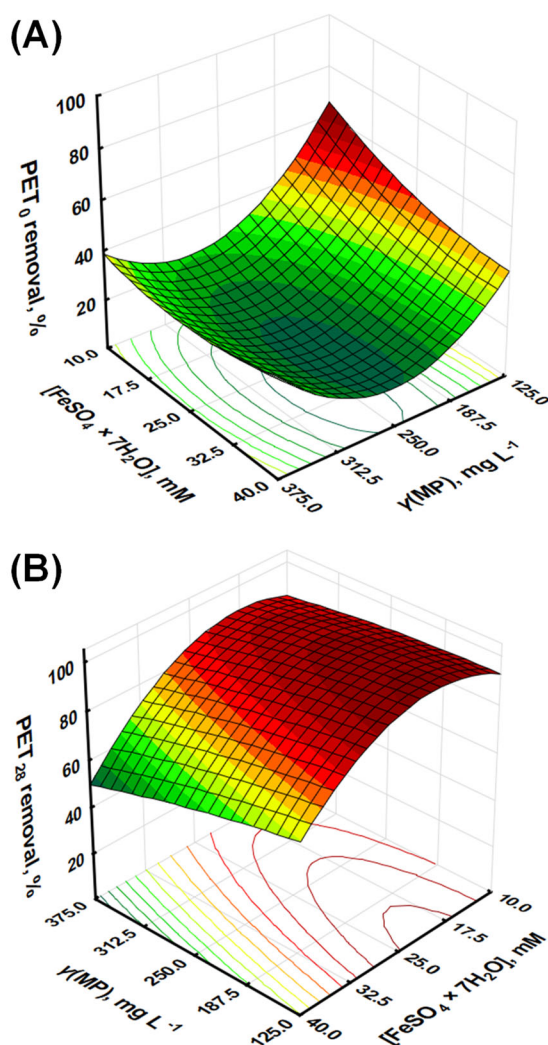


Figure 1. Response surface models for the removal effectiveness of (A) PET₀ and (B) PET₂₈ by response surface modeling.

Statistically, the model showed excellent goodness-of-fit, with an R^2 of 0.9895, an adjusted R^2 of 0.9721, and a predicted R^2 of 0.8791. These values indicate that the model explains a significant portion of the variability in the data and can predict new observations with reasonable accuracy. The F -value of the model was 56.80, with a p -value of 0.0036, suggesting a statistically significant relationship between the variables and the response (Table 2).

Table 2. Analysis of variance (ANOVA) of RSM models R_1 and R_2 predicting removal effectiveness of PET_0 and PET_{28} , respectively, by Fe^{2+}/H_2O_2 process.

Factor (Coded)	Statistical Analysis									
	SS		df		MSS		F		p	
	Y_1	Y_2	Y_1	Y_2	Y_1	Y_2	Y_1	Y_2	Y_1	Y_2
Model	2023.89	2241.41	5	5	404.78	448.28	56.80	44.72	0.0036 *	0.0051 *
X_1	319.89	312.19	1	1	319.89	312.19	44.89	31.14	0.0068 *	0.0114 *
X_1^2	1307.48	4.87	1	1	1307.48	4.87	183.46	0.49	0.0009 *	0.5361
X_2	171.31	1232.09	1	1	171.31	1232.09	24.04	122.91	0.0162 *	0.0016 *
X_2^2	66.20	632.97	1	1	66.20	632.97	9.29	63.14	0.0555	0.0042 *
$X_1 \times X_2$	159.01	59.29	1	1	159.01	59.29	22.31	5.91	0.0180 *	0.0932
Residual	21.38	30.07	3	3	7.13	10.02				
Total	2045.27	2271.49	8	8						

* $p < 0.05$ means that model or model term is significant.

The further judgment of RSM models accuracy, i.e., adequacy of model fitting to empirical values and corresponding lack of fit, includes the so-called “residual diagnostic” (RD), which is based on normal probability test, Levene’s test, and constant variance test. The RD for the Y_1 model revealed that: (i) there were no violations in the assumptions that the errors were normally distributed and independent of each other, (ii) the error variances were homogeneous, and (iii) residuals were independent, while the demonstration of performed graphical analysis of RD is given in Figure S1 (Supplementary Material). Taking into account the above-given information on Y_1 , it can be concluded that the derived model can be used hereinafter as a tool to enlighten the influence of studied parameters on Fenton treatment effectiveness and provide more information on occurring mechanisms and process chemistry. The evaluation of the influence of individual model terms representing process parameters was performed. As seen from Table 2, the individual linear model terms have p -values below 0.05, i.e., X_1 ($p = 0.0068$) and X_2 ($p = 0.0162$), indicating that process variables represented by both terms are significantly related to the removal of PET_0 MPs. Quadratic model term X_1^2 , representing PET_0 mass concentration, was also found to be highly significant, with a p -value of 0.0009, as was the model term representing the interaction between PET_0 mass concentration and iron catalyst concentration ($p = 0.0180$) (Table 2). The latter clearly indicates the necessity for applying the RSM approach to investigate the influence of the studied parameters on the effectiveness of MP removal by the Fenton process instead of the commonly applied “one-parameter-at-the-time” approach. Such an approach does not consider mutual interactions between studied parameters and may provide misleading information [27]. As can be seen from Equation (1), the negative coefficients associated with the linear terms, i.e., X_1 and X_2 , suggest that an increase in either the concentration of PET MPs or Fe^{2+} individually decreases the removal efficiency. The negative impact of the increase of PET MP concentrations is unsurprising, as the removal capacity of the combined Fenton and coagulation process diminishes as the concentration of MPs increases. The negative impact of X_2 is somewhat surprising, as one would expect that higher concentrations of Fe^{2+} would produce more $\bullet OH$. However, an excess amount of Fe^{2+} may lead to the production of less reactive species, such as hydroperoxyl radicals ($HO_2\bullet$) or peroxide ions (O_2^{2-}) through the Fenton–Weiss or the Haber–Weiss reactions. In addition, recombination reactions between the $\bullet OH$ can become more significant [28,29]. Interestingly, the interaction term between X_1 and X_2 ($X_1 \times X_2$) had a positive coefficient,

implying that a simultaneous increase in the concentrations of both PET microplastics and Fe^{2+} enhances the removal efficiency. This synergy could potentially stem from the need for a balanced ratio between PET concentration and Fe^{2+} for optimal removal effectiveness during oxidation and the post-oxidation coagulation step, as a higher concentration of Fe^{2+} would lead to better removal effectiveness. Likewise, at higher concentrations, it is more likely that growing hydrated iron oxide species will entrap PET MPs. The quadratic terms of X_1 and X_2 , i.e., X_1^2 and X_2^2 (although the latter is not highly significant for the derived Y_1 model), further highlight the complexity of the system. Both terms showed positive coefficients, suggesting a parabolic relationship between the variables and the response. This indicates the existence of an optimum concentration for both parameters, where any deviation would result in a decrease in removal efficiency. These insights underline the intricate interdependencies of the variables in the Fenton process for microplastic removal, emphasizing the need for a well-balanced reaction system. An increase in Fe^{2+} concentration or PET concentration individually leads to reduced removal, while a joint increase improves it. Furthermore, the quadratic terms suggest an optimal concentration for each parameter, stressing the importance of fine-tuning the reaction conditions to achieve maximum microplastic removal.

Taking into account the analogy used in Y_1 construction, the response equation (Y_2) fitted from the data in Table S2 (Supplementary Information) for the removal of PET_{28} is shown in Equation (3):

$$Y_2 = 94.22 - 7.21X_1 - 14.3 X_2 - 3.85 X_1 \times X_2 - 1.56X_1^2 - 17.79X_2^2 \quad (3)$$

The ANOVA results for the R_2 model indicate a good fit for the model ($R^2 = 0.9868$, adjusted $R^2 = 0.9647$, predicted $R^2 = 0.8542$), with the F -value (44.71) and p -value (0.0051) providing evidence of a statistically significant relationship between the variables and the response (Table 2). The RD for the Y_2 model is presented graphically in Figure S1 (Supplementary Materials). Based on the results, the conclusions are similar to that above for R_1 ; thus, Y_2 can be used as a tool to enlighten the influence of the studied parameters on Fenton treatment effectiveness for treating PET_{28} samples. In the following step, the significance of the individual model terms is characterized. The p -values for X_1 (0.0114) and X_2 (0.0016) are below 0.05, indicating significant main effects, while the p -value for $X_1 \times X_2$ (0.0932) suggests a possible interaction effect at the 10% level. The quadratic terms show a significant effect for X_2^2 ($p = 0.0042$), while X_1^2 ($p = 0.5362$) does not seem to be significant (Table 2). From the given second-order polynomial model, i.e., Y_2 , simulating the removal of UV-weathered PET microplastics over 28 consecutive days, we saw a somewhat different pattern of variable effects compared to the non-weathered PET microplastics (Y_1). Similar to the model for Y_1 , the negative coefficients for the linear terms of X_1 and X_2 (-7.21 for X_1 and -14.33 for X_2) suggest that an increase in either the concentration of PET microplastics or Fe^{2+} individually results in a decrease in removal efficiency. This effect appears to be more pronounced for UV-weathered PET, especially with regards to the Fe^{2+} concentration (X_2), as indicated by the larger negative coefficient (-14.33 for Y_2 compared to -5.34 for Y_1). The interaction term ($X_1 \times X_2$) was also negative (-3.85), implying that a simultaneous increase in the concentrations of PET microplastics and Fe^{2+} leads to a further decrease in removal efficiency, in contrast to the non-weathered case, where this interaction was positive. This suggests that the synergistic effect observed for the non-weathered PET microplastics does not occur for the UV-weathered PET microplastics or might even be reversed. The quadratic terms (X_1^2 and X_2^2) were also negative (-1.56 for X_1^2 and -17.79 for X_2^2), which suggests a downward-opening parabola and indicates that removal efficiency decreases at both low and high concentrations of the variables, with a maximum at some intermediate concentration. This is similar to the pattern observed for non-weathered PET microplastics, although the effect appears to be more pronounced for UV-weathered PET, especially for X_2 ($[\text{Fe}^{2+}]$).

Table 3 provides a comparative literature review of MP removal by various advanced oxidation processes. It should be noted that research on MPs, including their removal by

various methods, is a “hot topic”; thus, many studies are available (Figure 2). However, there are no standards for the systematic approach; thus, different MPs, in both type and size, are studied, while conditions varied greatly, even between the same/similar processes, as well as experimental set-up configurations and targeted environmental standards for monitoring MP removal. Additionally, many studies are not research articles but reviews tackling MP occurrence, fate, behavior, and remediation methods. In addition, studies on PET removal by advanced oxidation processes are rather scarce (Figure 2).

Table 3. A comparison of microplastic (MP) removal by various advanced oxidation treatments.

Type of MPs Studied	Treatment Method	Treatment Conditions	MPs Removal Extent	Ref.
Polyethylene (PE)	Fenton process	[Fe ²⁺] = 4 mM, [H ₂ O ₂] = 200 mM, acidic pH, 140 °C, 12 h	75.6% mineralization	[30]
Polystyrene (PS)	Fenton process	[Fe ³⁺] = 0–0.63 mM, [H ₂ O ₂] = 0–176 mM, pH 2, 250 W Xe lamp, 250 min	99% mineralization	[31]
Polystyrene (PS)	Ozonation	[O ₃] = 4.1 mg L ⁻¹ , 240 min	42.7% mineralization	[32]
Polystyrene (PS)	Fenton process	[Fe ³⁺] = 10 mg L ⁻¹ , [H ₂ O ₂] = 1000 mg L ⁻¹ , pH 3; T = 80 °C, 7.5 h	70% mineralization	[33]
Polystyrene (PS)	Photocatalysis	UV-A (354 nm), TiO ₂ @SiC foam, natural pH, 7 h	35% mineralization	[34]
Polyethylene terephthalate (PET)	Photocatalysis	300 W Xe lamp, Bi ₂ O ₃ @N-TiO ₂ , pH 9, 48 h	10.23% mass loss	[35]
Polyethylene terephthalate (PET)	Photocatalysis	CdS/CeO ₂ (wt. CdS 10%), [HSO ₅ ⁻] = 3 mM, 6 h	~94% mass loss	[36]
Polyethylene terephthalate (PET)	Photocatalysis	Co-CeO ₂ , [HSO ₅ ⁻] = 3 mM, [H ₂ O ₂] = 3 mM, 6 h	~92% mass loss	[37]

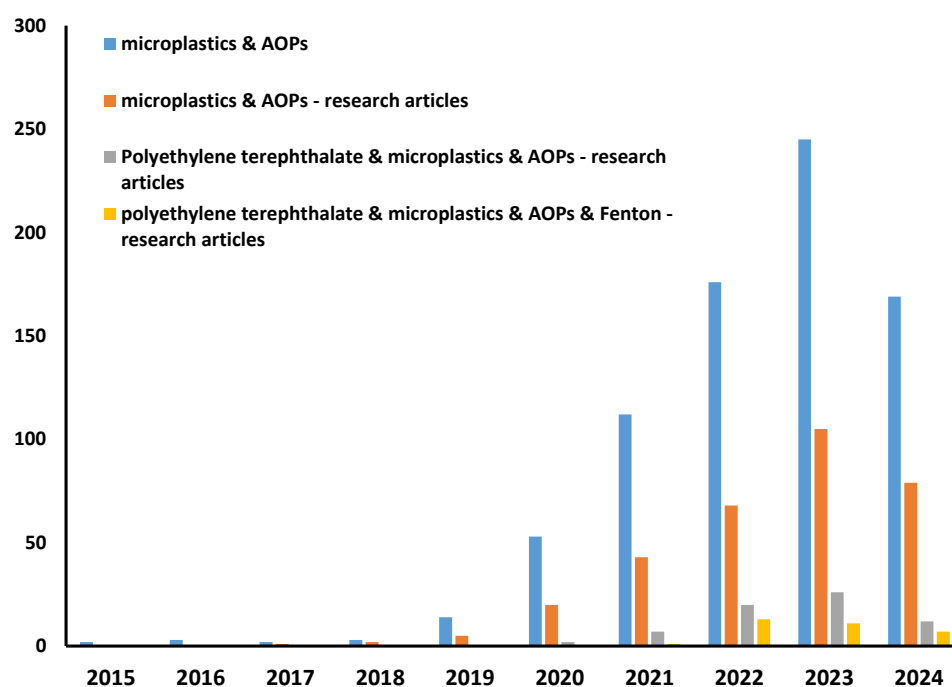


Figure 2. Results of literature search using terms “microplastics”, “AOPs”, “polyethylene terephthalate”, and “Fenton” (Science Direct base, 16 April 2024).

Accordingly, we have compared available data obtained from studies where Fenton processes (at different conditions) were applied for the treatment of different MP types, including PET, targeting mineralization degrees as the evaluation parameter for process effectiveness due to the easier comparison (Table 3). As can be seen, the Fenton process was shown to be rather powerful in mineralizing MP pollution; between 70 and 99% were

obtained depending on the conditions of the Fenton process and type and presence of additional treatment empowerment (e.g., irradiation, heat). Similarly, high removal rates were recorded and thereafter modeled via the RSM approach in our study as well, with 68 and 98% PET removals for pristine and aged samples, respectively (Figure 1). Another process with promising PET removal was the hybrid photocatalysis process, empowered by the addition of strong oxidants, where over 90% of mass losses were recorded for PET MPs (Table 3). However, practical and economic constraints may favor Fenton treatment over photocatalysis; irradiation is energy-consumptive, while the removal of fine powder from nano-scale photocatalysts may also increase the cost of treatment.

3.2. X-ray Photoemission Spectroscopy Analysis of the PET MPs

To better understand the changes induced in PET MPs by UV weathering and the Fenton process, we performed X-ray photoemission spectroscopy analyses. First, pristine PET₀ and UV-weathered PET₂₈ samples were analyzed. As can be seen in Table 4, deconvoluted C 1s and, consequently, integrated XPS spectra (spectra provided in Figure S2, Supplementary Information) reveal changes in the composition of the UV-weathered PET₂₈ samples. A decrease in the relative areas, i.e., the amount of the C-O-C/C-OH bonds and O-C=O bonds, implies that UV-weathering has effectively cleaved ester bonds within the polymer and has additionally led to a loss of the terminal -OH and -COOH groups from the ends of the PET macromolecular chains [28]. Conversely, the increasing areas of the peaks corresponding to C=C and conjugated π - π systems after UV-weathering reveals the formation of unsaturated carbon-carbon bonds and enhanced π - π interactions. Decarboxylation and subsequent chain scission result in the formation of smaller oligomers, which have fewer degrees of freedom. In turn, these smaller fragments have fewer ways to rotate around their bonds, which promotes π - π stacking interactions [29]. Moreover, the chain scission process creates oligomer radicals that can cross-link, thus explaining the increase in the amount of C-C bonds. The UV-weathered PET sample is, thus, more likely to undergo reactions with \bullet OH radicals due to a greater abundance of unsaturated C=C bonds and saturated C-C, C-H bonds, whereas less reactive C-OH and O-C=O, which may, in particular, inhibit the Fenton reaction, are less abundant.

Table 4. Areas corresponding to the deconvoluted C 1s core level peaks in X-ray photoemission spectroscopy (XPS) analysis for untreated samples PET₀ and PET₂₈.

Identified Functional Groups and Interactions	PET ₀ , %	PET ₂₈ , %
C=C	38.80	40.64
C-O-C, C-OH	21.73	19.73
O-C=O	17.38	16.48
π - π	2.70	2.83
C-C, C-H	19.40	20.32

XPS analysis of Fenton-treated samples, namely those corresponding to the maximum X₁ and X₂-coded variable values, i.e., initial PET MP concentration and Fe²⁺ concentration, were analyzed by XPS; the results are shown in Table 5, and the spectra are provided in Supplementary Information. These two experiments have a marked difference in the achieved removal extent, as evident in Figure 1.

A stark contrast in the composition of the post-Fenton treatment was evident. Immediately, we observed that UV-weathered PET was further oxidized to a much greater extent in the Fenton process, which was clearly demonstrated by greater contributions of the C-O-C and C-OH bonds in the PET₂₈ sample and, in turn, a much lower C=C content. However, pristine PET was also oxidized to a greater extent, i.e., the contribution of the O-C=O bonds was much greater for the Fenton-treated PET₀ sample (Table 5). The growing contribution of the O-C=O moiety for the Fenton-treated PET₀ sample implies effective fragmentation of the PET MPs. Additionally, \bullet OH facilitates the formation of cross-linked

moieties, as the contributions of the C-C and C-H groups more than doubled for PET₀ alone. However, the greater carboxyl moiety content of the PET₀ samples post-Fenton treatment gives an insight into why the removal effectiveness is lower in relation to PET₂₈. The greater abundance of oligomers with carboxyl groups more than likely leads to the formation of stable and inactive Fe³⁺ chelate complexes, thus greatly reducing the effectiveness of the Fenton process [38,39]. XPS analysis and deconvolution of the Fe 2p_{3/2} core-level spectra support this notion.

Table 5. Areas corresponding to the deconvoluted C 1s core level peaks in X-ray photoemission spectroscopy (XPS) analysis for Fenton-treated samples PET₀ and PET₂₈.

Identified Functional Groups and Interactions	PET ₀ , %	PET ₂₈ , %
C=C	35.80	15.80
C-O-C, C-OH	8.70	46.48
O-C=O	30.5	8.81
π - π	2.49	1.10
C-C, C-H	43.57	21.69

4. Conclusions

The response surface models indicate a complex relationship between the removal effectiveness of PET microplastics and the concentrations of PET MPs and Fe²⁺. The effects of these variables appear to be markedly different for non-weathered and UV-weathered PET. For non-weathered PET, there seems to be a synergistic effect between PET and Fe²⁺ concentration, which is not observed for UV-weathered PET. Also, the effect of Fe²⁺ concentration appears to be more pronounced for UV-weathered PET. These findings suggest that weathering may change the physicochemical properties of PET microplastics, altering their reactivity in the Fenton process. Indeed, XPS analysis has revealed that UV-weathering predisposes PET MPs to Fenton degradation; specifically, the greater abundance of C=C and C-C bonds facilitates more effective degradation by OH radicals. In addition, the abundance of O-C=O decreases, which in turn does not lead to the formation of inactive Fe³⁺ chelate complexes. Therefore, it is crucial to take into account the potential effects of environmental weathering when developing and optimizing microplastic removal strategies. Further experimental research is needed to fully understand these effects; however, these results indicate that the Fenton treatment is a viable means for the removal of PET MPs. In addition, these findings, especially that UV weathering has enhanced the effectiveness of the Fenton process, have far-reaching implications for the treatment processes concerned with the removal of polyester-based microplastics.

Supplementary Materials: The following supporting information can be downloaded at: <https://www.mdpi.com/article/10.3390/pr12040844/s1>, Table S1. Full-factorial experimental plan for the removal of pristine PET MPs (PET₀) with the Fenton process; Table S2. Full-factorial experimental plan for the removal of PET MPs obtained from UV-weathered PET for 28 days (PET₂₈) with the Fenton process; Figure S1. Deconvoluted XPS C 1s spectra for (A) PET₀ MPs, and (B) PET₂₈ MPs. Figure S2. Deconvoluted XPS C 1s spectra for samples (A) PET₀ MPs, and (B) PET₂₈ MPs corresponding to experiment #8 in Tables S1 and S2, respectively, after the Fenton treatment. Figure S3. Deconvoluted XPS Fe 2p_{3/2} core-level spectra for samples (A) PET₀ MPs, and (B) PET₂₈ MPs corresponding to experiment #8 in Tables S1 and S2, respectively, after the Fenton treatment.

Author Contributions: Conceptualization, A.L.B. and M.K.; methodology, M.K. and Z.K.; software, M.K.; validation, M.K., H.K., B.G. and A.L.B.; formal analysis, M.K. and Z.K.; investigation, A.T., S.T., J.P.Z., and A.P.; resources, B.G. and A.L.B.; data curation, M.K. and A.T.; writing—original draft preparation, M.K.; writing—review and editing, A.L.B.; visualization, M.K.; supervision, A.L.B.; project administration, A.L.B.; funding acquisition, A.L.B. All authors have read and agreed to the published version of the manuscript.

Funding: This research was funded by the Croatian Science Foundation, grant number IP-2020-02-6033.

Data Availability Statement: The data will be available upon reasonable request.

Conflicts of Interest: The authors declare no conflicts of interest.

References

1. Andrady, A.L. Microplastics in the marine environment. *Mar. Pollut. Bull.* **2011**, *62*, 1596–1605. [CrossRef] [PubMed]
2. Plastics—The Facts. 2022. Available online: <https://plasticseurope.org/knowledge-hub/plastics-the-facts-2022/> (accessed on 12 March 2024).
3. Revel, M.; Châtel, A.; Mouneyrac, C. Micro(nano)plastics: A threat to human health? *Curr. Opin. Environ. Sci. Health* **2018**, *1*, 17–23. [CrossRef]
4. Bhuyan, M.S. Effects of Microplastics on Fish and in Human Health. *Front. Environ. Sci.* **2022**, *10*, 827289. [CrossRef]
5. Yin, X.; Wu, J.; Liu, Y.; Chen, X.; Xie, C.; Liang, Y.; Li, J.; Jiang, Z. Accumulation of microplastics in fish guts and gills from a large natural lake: Selective or non-selective? *Environ. Pollut.* **2022**, *309*, 119785. [CrossRef] [PubMed]
6. Wright, S.L.; Kelly, F.J. Plastic and Human Health: A Micro Issue? *Environ. Sci. Technol.* **2017**, *51*, 6634–6647. [CrossRef] [PubMed]
7. Wright, S.L.; Thompson, R.C.; Galloway, T.S. The physical impacts of microplastics on marine organisms: A review. *Environ. Pollut.* **2013**, *178*, 483–492. [CrossRef] [PubMed]
8. Li, Z.; Chang, X.; Hu, M.; Fang, J.K.-H.; Sokolova, I.M.; Huang, W.; Xu, E.G.; Wang, Y. Is microplastic an oxidative stressor? Evidence from a meta-analysis on bivalves. *J. Hazard. Mater.* **2022**, *423*, 127211. [CrossRef]
9. Adedirán, G.A.; Cox, R.; Jürgens, M.D.; Morel, E.; Cross, R.; Carter, H.; Pereira, M.G.; Read, D.S.; Johnson, A.C. Fate and behaviour of Microplastics (>25 µm) within the water distribution network, from water treatment works to service reservoirs and customer taps. *Water Res.* **2024**, *255*, 121508. [CrossRef] [PubMed]
10. Visentin, E.; Manuelian, C.L.; Niero, G.; Benetti, F.; Perini, A.; Zanella, M.; Pozza, M.; De Marchi, M. Characterization of microplastics in skim-milk powders. *J. Dairy Sci.* **2024**. [CrossRef]
11. Silva, D.M.; Almeida, C.M.R.; Guardioli, F.A.; Pereira, R.; Rodrigues, S.M.; Ramos, S. Uncovering microplastics contamination in canned seafood. *Food Chem.* **2024**, *448*, 139049. [CrossRef]
12. Syamsu, D.A.; Deswati, D.; Syafrizayanti, S.; Putra, A.; Suteja, Y. Presence of microplastics contamination in table salt and estimated exposure in humans. *Glob. J. Environ. Sci. Manag.* **2024**, *10*, 205–224.
13. Espiritu, E.Q.; Pauco, J.L.R.; Bareo, R.S.; Palaypayon, G.B.; Capistrano, H.A.M.; Jabar, S.R.; Coronel, A.S.O.; Rodolfo, R.S.; Enriquez, E.P. Microplastics contamination in selected staple consumer food products. *J. Food Sci. Technol.* **2024**. [CrossRef]
14. Rochman, C.M.; Hoh, E.; Kurobe, T.; Teh, S.J. Ingested plastic transfers hazardous chemicals to fish and induces hepatic stress. *Sci. Rep.* **2013**, *3*, 3263. [CrossRef]
15. Teuten, E.L.; Saquing, J.M.; Knappe, D.R.U.; Barlaz, M.A.; Jonsson, S.; Björn, A.; Rowland, S.J.; Thompson, R.C.; Galloway, T.S.; Yamashita, R.; et al. Transport and release of chemicals from plastics to the environment and to wildlife. *Philos. Trans. R. Soc. B Biol. Sci.* **2009**, *364*, 2027–2045. [CrossRef]
16. Zettler, E.R.; Mincer, T.J.; Amaral-Zettler, L.A. Life in the “Plastisphere”: Microbial Communities on Plastic Marine Debris. *Environ. Sci. Technol.* **2013**, *47*, 7137–7146. [CrossRef] [PubMed]
17. Ho, W.K.; Law, J.C.F.; Zhang, T.; Leung, K.S.Y. Effects of Weathering on the Sorption Behavior and Toxicity of Polystyrene Microplastics in Multi-solute Systems. *Water Res.* **2020**, *187*, 116419. [CrossRef]
18. Carr, S.A.; Liu, J.; Tesoro, A.G. Transport and fate of microplastic particles in wastewater treatment plants. *Water Res.* **2016**, *91*, 174–182. [CrossRef] [PubMed]
19. Dos Santos, N.d.O.; Busquets, R.; Campos, L.C. Insights into the removal of microplastics and microfibres by Advanced Oxidation Processes. *Sci. Total Environ.* **2023**, *861*, 160665. [CrossRef] [PubMed]
20. Bule Možar, K.; Miloloža, M.; Martinjak, V.; Cvetnić, M.; Kušić, H.; Bolanča, T.; Kučić Grgić, D.; Ukić, Š. Potential of Advanced Oxidation as Pretreatment for Microplastics Biodegradation. *Separations* **2023**, *10*, 132. [CrossRef]
21. Babuponnusami, A.; Muthukumar, K. A review on Fenton and improvements to the Fenton process for wastewater treatment. *J. Environ. Chem. Eng.* **2014**, *2*, 557–572. [CrossRef]
22. Kusic, H.; Koprivanac, N.; Srsan, L. Azo dye degradation using Fenton type processes assisted by UV irradiation: A kinetic study. *J. Photochem. Photobiol. A Chem.* **2006**, *181*, 195–202. [CrossRef]
23. Papac Zjačić, J.; Tonković, S.; Pulitika, A.; Katančić, Z.; Kovačić, M.; Kušić, H.; Hrnjak Murgić, Z.; Lončarić Božić, A. Effect of Aging on Physicochemical Properties and Size Distribution of PET Microplastic: Influence on Adsorption of Diclofenac and Toxicity Assessment. *Toxics* **2023**, *11*, 615. [CrossRef]
24. Dopar, M.; Kusic, H.; Koprivanac, N. Treatment of simulated industrial wastewater by photo-Fenton process. Part I: The optimization of process parameters using design of experiments (DOE). *Chem. Eng. J.* **2011**, *173*, 267–279. [CrossRef]
25. Kovacic, M.; Salaeh, S.; Kusic, H.; Suligoj, A.; Kete, M.; Fanetti, M.; Stangar, U.L.; Dionysiou, D.D.; Bozic, A.L. Solar-driven photocatalytic treatment of diclofenac using immobilized TiO₂-based zeolite composites. *Environ. Sci. Pollut. Res.* **2016**, *23*, 17982–17994. [CrossRef]
26. Tomic, A.; Cvetnic, M.; Kovacic, M.; Kusic, H.; Karamanis, P.; Bozic, A.L. Structural features promoting adsorption of contaminants of emerging concern onto TiO₂ P25: Experimental and computational approaches. *Environ. Sci. Pollut. Res.* **2022**, *29*, 87628–87644. [CrossRef]

27. Chong, M.N.; Jin, B.; Chow, C.W.K.; Saint, C. Recent developments in photocatalytic water treatment technology: A review. *Water Res.* **2010**, *44*, 2997–3027. [[CrossRef](#)]
28. Edge, M.; Wiles, R.; Allen, N.S.; McDonald, W.A.; Mortlock, S.V. Characterisation of the species responsible for yellowing in melt degraded aromatic polyesters—I: Yellowing of poly(ethylene terephthalate). *Polym. Degrad. Stab.* **1996**, *53*, 141–151. [[CrossRef](#)]
29. Hermann, J.; Alfè, D.; Tkatchenko, A. Nanoscale π - π stacked molecules are bound by collective charge fluctuations. *Nat. Commun.* **2017**, *8*, 14052. [[CrossRef](#)]
30. Hu, K.; Zhou, P.; Yang, Y.; Hall, T.; Nie, G.; Yao, Y.; Duan, X.; Wang, S. Degradation of Microplastics by a Thermal Fenton Reaction. *ACS ES&T Eng.* **2022**, *2*, 110–120.
31. Feng, H.-M.; Zheng, J.-C.; Lei, N.-Y.; Yu, L.; Kong, K.H.-K.; Yu, H.-Q.; Lau, T.-C.; Lam, M.H.W. Photoassisted Fenton Degradation of Polystyrene. *Environ. Sci. Technol.* **2011**, *45*, 744–750. [[CrossRef](#)]
32. Li, Y.; Li, J.; Ding, J.; Song, Z.; Yang, B.; Zhang, C.; Guan, B. Degradation of nano-sized polystyrene plastics by ozonation or chlorination in drinking water disinfection processes. *Chem. Eng. J.* **2022**, *427*, 131690. [[CrossRef](#)]
33. Ortiz, D.; Munoz, M.; Nieto-Sandoval, J.; Romera-Castillo, C.; de Pedro, Z.M.; Casas, J.A. Insights into the degradation of microplastics by Fenton oxidation: From surface modification to mineralization. *Chemosphere* **2022**, *309*, 136809. [[CrossRef](#)]
34. Allé, P.H.; Garcia-Muñoz, P.; Adouby, K.; Keller, N.; Robert, D. Efficient photocatalytic mineralization of polymethylmethacrylate and polystyrene nanoplastics by $\text{TiO}_2/\beta\text{-SiC}$ alveolar foams. *Environ. Chem. Lett.* **2021**, *19*, 1803–1808. [[CrossRef](#)]
35. Zhou, D.; Wang, L.; Zhang, F.; Wu, J.; Wang, H.; Yang, J. Feasible Degradation of Polyethylene Terephthalate Fiber-Based Microplastics in Alkaline Media with $\text{Bi}_2\text{O}_3@\text{N-TiO}_2$ Z-Scheme Photocatalytic System. *Adv. Sustain. Syst.* **2022**, *6*, 2100516. [[CrossRef](#)]
36. Wan, Y.; Wang, H.; Liu, J.; Liu, X.; Song, X.; Zhou, W.; Zhang, J.; Huo, P. Enhanced degradation of polyethylene terephthalate plastics by CdS/CeO_2 heterojunction photocatalyst activated peroxymonosulfate. *J. Hazard. Mater.* **2023**, *452*, 131375. [[CrossRef](#)]
37. Wan, Y.; Wang, H.; Liu, J.; Li, J.; Zhou, W.; Zhang, J.; Liu, X.; Song, X.; Wang, H.; Huo, P. Removal of polyethylene terephthalate plastics waste via Co-CeO_2 photocatalyst-activated peroxymonosulfate strategy. *Chem. Eng. J.* **2024**, *479*, 147781. [[CrossRef](#)]
38. Timoshnikov, V.A.; Kobzeva, T.V.; Polyakov, N.E.; Kontoghiorghes, G.J. Inhibition of Fe^{2+} - and Fe^{3+} - induced hydroxyl radical production by the iron-chelating drug deferiprone. *Free Radic. Biol. Med.* **2015**, *78*, 118–122. [[CrossRef](#)]
39. Milovac, N.; Juretic, D.; Kusic, H.; Dermadi, J.; Bozic, A.L. Photooxidative degradation of aromatic carboxylic acids in water: Influence of hydroxyl substituents. *Ind. Eng. Chem. Res.* **2014**, *53*, 10590–10598. [[CrossRef](#)]

Disclaimer/Publisher's Note: The statements, opinions and data contained in all publications are solely those of the individual author(s) and contributor(s) and not of MDPI and/or the editor(s). MDPI and/or the editor(s) disclaim responsibility for any injury to people or property resulting from any ideas, methods, instructions or products referred to in the content.